THE JOURNAL OF BIOLOGICAL CHEMISTRY
Vol. 273, No. 44, Issue of October 30, pp. 28576–28582, 1998

Printed in U.S.A.

Crystal Structure of Monoclonal 6B5 Fab Complexed with Phencyclidine*

(Received for publication, June 17, 1998)

Kap Lim‡, S. Michael Owens§, Larry Arnold¶, James C. Sacchettini‡‖, and D. Scott Linthicum‡**

From the ‡Center for Structural Biology, Department of Biochemistry and Biophysics, Texas A&M University, College Station, Texas, 77843, the §Department of Pharmacology and Toxicology, College of Medicine, University of Arkansas for Medical Sciences, Little Rock, Arkansas 72205, and the ¶Department of Microbiology and Immunology, University of North Carolina, Chapel Hill, North Carolina 27514

The crystal structure of monoclonal antibody (mAb) 6B5 Fab fragment complexed with 1-(1-phenylcyclohexyl)piperidine (PCP or phencyclidine) was determined at 2.2-Å resolution. 6B5 was originally produced from a mouse immunized with a phencyclidine analogue hapten 5-[*N*-(1′phenylcyclohexyl)amino]pentanoic acid conjugated to bovine serum albumin. This mAb was selected for further study because of its high affinity (K_d = 2×10^{-9} M/liter) for PCP and usefulness in reversing PCP-induced central nervous system toxicity in laboratory animals. The dominant feature of the 6B5 Fab·PCP complex is the deep binding site and hydrophobic nature of the interaction. The ligand binding pocket of 6B5 Fab has numerous aromatic side chains, as compared with other known Fab structures. The most notable feature of the binding site is a Trp at position 97H (H-chain), and the side chain of this residue appears to act as a hydrophobic umbrella on the ligand in the antigen binding pocket. There are only two other known Fabs found with a Trp at the 97H position in complementarity determining region (CDR) H3, but they do not play a major role in the interaction with their respective antigens; in both Fab TE33 and R6.5 the Trp 97H side chain is positioned away from the bound antigen. Comparison of the CDR residues of 6B5 with other Fab structures with similar CDR sizes and amino acid compositions reveals a number of important patterns of residue substitutions that appear to be critical for specific PCP ligand interactions.

Crystallographic determinations of antigen binding fragments (Fab)[1] derived from human and mouse immunoglobulins (Ig) have shown that the antigen binding pocket is created by six polypeptide loops or so-called complementarity determining regions (CDR) at the *en face* region of the Fab (1–3). The CDR structures are formed by the anti-parallel β-strand turns of the variable regions of light and heavy polypeptide chains. The favorable contacts between specific CDR amino acids of the antibody and the antigen epitopes accounts for the fine specificity of the interaction. Although most antibodies made against small ligand or drug antigens exhibit precise stereospecific interactions, it is not uncommon for some antibodies to bind to analogues or drug family members that are structurally related due to the position and orientation of specific intermolecular contacts.

Phencyclidine (1-(1-phenylcyclohexyl)piperidine, or PCP) and related arylcyclohexylamines have been shown to be potent dissociative psychotropic agents (4, 5). PCP has direct interactions with receptors for several central nervous system neurotransmitters, including the *N*-methyl-D-aspartate gated ion-channel complex (6) and the dopamine reuptake transporter (7, 8). The molecular features of PCP-like arylcyclohexylamines which are important for binding to the PCP binding site have been studied by generation of a series of polyclonal rabbit antibodies and mouse monoclonal antibodies (mAbs) to PCP-like haptens and related analogues (9, 10). By comparing the relative reactivity of various arylcyclohexylamine drugs in a [^{3}H]PCP radioimmunoassay with their relative potencies for PCP receptor binding in central nervous system membranes and central nervous system drug discrimination assays in rats, it was determined that 5-[*N*-(1′phenylcyclohexyl)amino]pentanoic acid (PCHAP) was a highly suitable ligand for generating antibodies that could recognize the pharmacologically active features required for arylcyclohexylamine binding to the PCP sites (9).

We report here the crystal structure of a Fab·PCP complex resolved at 2.2-Å resolution. The monoclonal antibody used in this study, clone 6B5, was produced against the phencyclidine-like hapten PCHAP (11). The structural knowledge of this Fab·PCP complex has aided our understanding of how this mAb is able to reverse acute PCP-induced central nervous system toxicity within minutes following intravenous administration (12). PCP is a well known drug of abuse and treatment of its overdose in humans is extremely problematic because there are no known antagonists and there is an extensive extravascular distribution and slow elimination of the drug in humans (13). Fab fragments of mAb 6B5 have been shown to be highly effective as an antibody-based treatment protocol for acute PCP toxicity in laboratory animals (11, 12). The structural knowledge of the 6B5 Fab·PCP complex will provide the basis for future 6B5 Fab and single-chain Fv (fragment variable) protein engineering experiments in an attempt to modify the antigenicity and enhance the pharmacokinetics, thereby providing a basis for clinical application of this antibody in the treatment of human patients with PCP-induced psychosis and toxicity.

* This work was supported by National Institutes of Health Grants R01 GM46535 (to D. S. L.), R01 DA07610, K02 DA00110 (to S. M. O), and R01 AI41240 (to J. C. S.); additional support was provided by the Welch Foundation (Houston, TX). The costs of publication of this article were defrayed in part by the payment of page charges. This article must therefore be hereby marked "*advertisement*" in accordance with 18 U.S.C. Section 1734 solely to indicate this fact.

The atomic coordinates and structure factors (code 2pcp) have been deposited in the Protein Data Bank, Brookhaven National Laboratory, Upton, NY.

‖ To whom correspondence may be addressed. Tel.: 409-862-7636; Fax: 409-862-7638; E-mail: sacchett@tamu.edu.

** To whom correspondence may be addressed: Tel.: 409-845-6981; Fax: 409-845-6980; E-mail: s-linthicum@tamu.edu.

[1] The abbreviations used are: Fab, antigen binding fragment; CDR, complementarity determining region; mAb, monoclonal antibody; PCP, 1-(1-phenylcyclohexyl)piperidine or phencyclidine; PCHAP, 5-[*N*-(1′phenylcyclohexyl)amino]pentanoic acid.

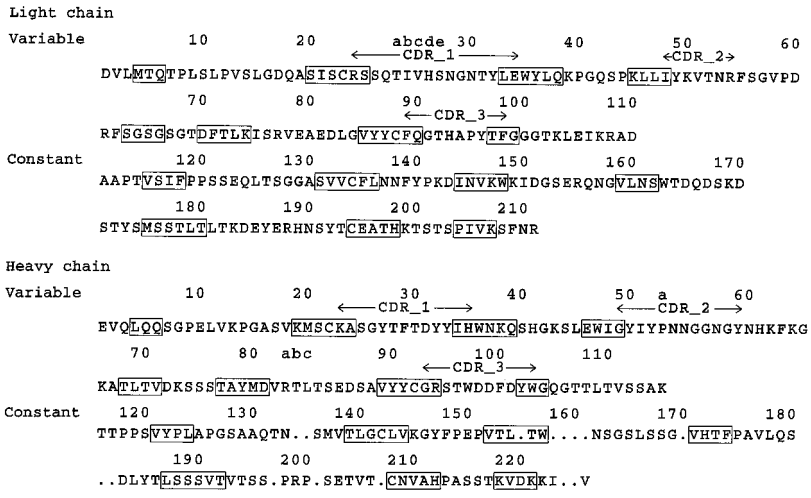

FIG. 1. **Amino acid sequences of 6B5 Fab.** The full sequences of 6B5 are shown to indicate the conserved β-strands (in *boxes*) of which Cα atoms were used in structure analysis. Also indicated are the amino acids of complementarity-determining regions (*CDRs*) at the antigen-binding site. Sequence numbers are assigned as in Kabat *et al.* (24).

EXPERIMENTAL PROCEDURES

Crystallization and Data Collection—The 6B5 Fab was produced and purified from whole IgG (G1, κ) as described previously (11). It was further purified in an affinity gel column conjugated with the PCHAP hapten, from which the 6B5 Fab was eluted with 0.1 M glycine-HCl buffer, pH 2.8. The affinity-purified Fab was concentrated and examined for purity with SDS-PAGE. At a concentration of 15 mg/ml, the 6B5 Fab was crystallized in 2.2 M ammonium sulfate and 0.1 M sodium acetate, pH 4.6, by the hanging drop crystallization method. The diffraction data were collected to 2.2-Å resolution with the MAC Science DIP2030 image plate system with double-focusing mirrors coupled to a Rigaku x-ray generator, using a copper rotating anode with a 5 μm nickel filter and a 0.5-mm x-ray beam collimator. The Denzo and Scalepack programs were used to autoindex, integrate, and scale multiple frames of data (14). Intensity data sets collected from two crystals gave a residual R_{merge} of 9.1% and were assigned the space group of $P1$. Summary of data collection and refinement statistics are presented in Table I.

Molecular Replacement and Structure Refinement—To obtain the molecular replacement solution for the 6B5 Fab·PCP complex, the 4–4-20 Fab (Protein Data Bank code 4fab) and HC19 Fab (Protein Data Bank code 1gig) structures were used as models in the search with the XPLOR program (15). These structures were chosen because of their common constant G1, κ chain sequences with 6B5. Using the 15.0–4.0-Å data, rotation search was performed separately for the variable and constant domain halves of the Fab. Because each variable or constant domain half consists of light and heavy chain subdomains, the Patterson correlation refinements were performed after the initial rotation search to improve their relative orientations. Top solutions from these refinements were used in the translation search. The size of the crystal lattice (Table I) indicated that there are two Fabs in the asymmetric unit with the solvent content of 45% (16). Because the space group is triclinic $P1$, no translation was necessary for the first variable domain pair, and three translation searches were performed for the remaining three Fab domain pairs of the asymmetric unit. The partial structure factors F_c for the first variable domain pair were computed and used in the translation search for the corresponding constant domain pair. Then a new set of F_c was computed for the translation search for the second variable domain pair. Again, a new set of F_c was computed and used in the translation search for the second constant domain pair. The 4–4-20 Fab model was used to determine the positions of the first three domain pairs but did not yield a solution for the second constant domain pair. The position of the latter was determined with the HC19 Fab model. The correlation coefficient improved progressively from 0.19 with only one variable domain pair positioned to 0.38 with all four components placed in the crystal lattice. The molecular replacement search with the 15.0–4.0-Å data also lowered the R factor, from 51.5 to 46.2%. Furthermore, the same solution was also obtained with another program, AMORE (17). Finally, the four Fab domain pairs were placed together in the crystal lattice and rigid body minimization was performed with the 8.0–3.0-Å data, and the R factor was further reduced to 44.7%.

For the structural refinements, omit maps computed from the 4,000 K-simulated annealing calculations with XPLOR were examined to ascertain the polypeptide tracing, especially for the CDR loops. Non-crystallographic restraints were not used on the two Fabs in the asymmetric unit during any part of the structure refinements. Structure visualization and model building tasks were performed with the O program (18). The amino acid substitutions were made in the 6B5 structure using the variable domain sequences for both L- and H-chains derived from the cDNA nucleotide sequencing of mRNA isolated from hybridoma cells (19) (Fig. 1). The constant domain sequences of 6B5 were not determined by cDNA sequencing. Because the constant domain gene families were found to be the same as the anti-lysozyme antibody HyHEL-5 (20), the HyHEL-5 structure was used for the electron density maps of the 6B5 diffraction data.

The position of the PCP molecule in the Fab binding site was determined with the $F_o - F_c$ difference map. The initial difference map indicated the presence of PCP at the center of the binding site. As the CDR loops with their side chains were built into the Fab structure with more certainty, the difference electron density of PCP became more defined. However, because PCP consists of three cyclic substituents, there was uncertainty about its true orientation in the binding site. This question was answered when the simulated annealing computation was performed with all the highest resolution data available (to 2.2 Å) and the difference electron density map revealed the PCP orientation (Fig. 2*A*). The published coordinates of the PCP crystal structure (21) were inserted in the model and another round of simulated annealed calculations were performed (Fig. 2*B*). The potential parameters for PCP were obtained from an automatic XPLOR parameter-generating program (available on the web site: http://alpha2.bmc.uu.S.E./hicup) (22, 23).

Ordered water molecules in the 6B5 Fab structure refinements, which used the 6.0–2.2-Å data, were chosen from the 3 σ peaks in the $F_o - F_c$ difference map with appropriate distance and interaction criteria, and symmetry consideration. After their inclusion in the model, their positions were again examined with the $2F_o - F_c$ map; any water molecules with less than 0.7 σ peaks in this map were rejected. The final R factor was 19.9%, with R_{free} of 28.6%. The refinement statistics are summarized in Table I. Coordinates of the 6B5 Fab structure have been deposited in Brookhaven Protein Data Bank (identification code 2PCP).

RESULTS

Overall Structure—The three-dimensional structure of 6B5 Fab complexed with PCP was determined to 2.2-Å resolution. 6B5 Fab possesses the typical immunoglobulin fold found in all antibody molecules, wherein the light (L) chain and heavy (H) chain form the variable (V) domain that contains the antigen-binding region, and constant (C) domain that have identical amino acid sequences within a gene class. Two Fab·PCP complexes were identified in the asymmetric unit of space group $P1$. They are positioned in opposite directions with the interface at the constant domain (Fig. 3). Amino acids of 1L to 211L of L-chain (216 residues) and of 1H to 226H of H-chain (215 residues) were assigned in both Fab of the asymmetric unit (Fig. 1). Amino acid sequence numbering scheme for Ig as described by Kabat *et al.* (24) is used in this report. Most of the

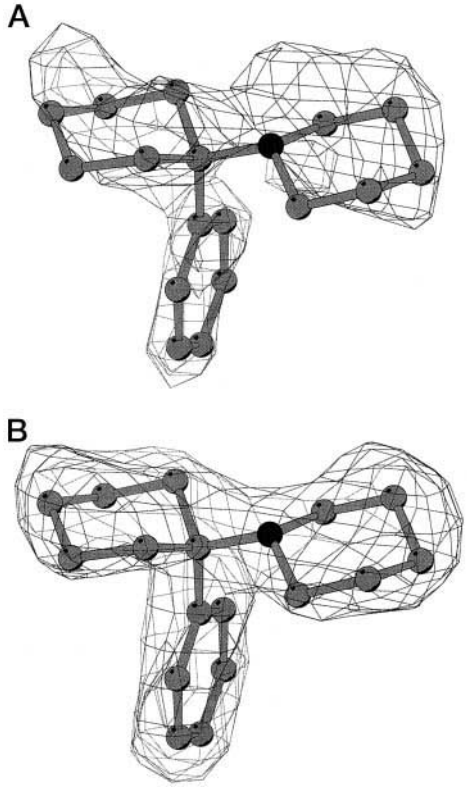

FIG. 2. **Electron density map of PCP from 6B5 Fab binding site at 2.2 Å resolution.** *A*, $F_o - F_c$ difference map of PCP contoured at 2.7 σ which indicated the proper orientation of PCP in the binding site. *B*, $2F_o - F_c$ map contoured at 1.0 σ after the inclusion of PCP in the structure. Molecular structures are drawn with the Molscript program (41).

structural elements are well defined and unambiguously assigned, including the PCP ligand. The two regions of relatively weak electron densities are amino acid residues 198L-203L in the constant L-chain domain and 127H-133H in the constant H-chain domain.

The structure of 6B5 was analyzed using Cα atoms of conserved β-strand residues, as indicated in Fig. 1 and shown in Table II. The Cα atoms of variable or constant domain of the heavy chain are rotated to superimpose on the corresponding Cα atoms of the light chain. The axis of this rotation between the two chains is termed *pseudodyad*. The *elbow angle* is computed with the two pseudodyads of the variable and constant domain pairs. The elbow angles are 143° for Fab 1, and 139° for Fab 2. These values deviate significantly from 180° but fall within the range of those of other Fabs surveyed, from 127 to 227° (25). Pseudodyads are more close to 180° for V domains than for C domains (Table II). In addition, molecular surface areas were computed with the probe radius of 1.7 Å (26). The buried surface area of the VL-VH interface is 1,309 Å^2 for Fab 1 (663 for VL and 646 for VH) and 1,299 Å^2 for Fab 2 (664 for VL and 635 for VH). These values of 6B5 are in the mid-range of those observed in other Fab structures (1,100 to 1,700 Å^2) (27) and comparable with the buried surface area of 1,375 Å^2 for the anti-fluorescein 4–4-20 Fab (28), the search model for 6B5. However, the elbow angle of 171° of 4–4-20 is much greater than that of 6B5.

The elbow angles of 6B5 Fab reflect the uneven positions of the V- and C-domains of L-chain relative to that found in the H-chain. The distances between the centers of mass for the Cα atoms of conserved β-strand residues (Fig. 1) are 39 Å for VL and CL, and 32 Å for VH and CH. The differences of these values between the two Fabs are within 1 Å. The elongation on the L-chain side causes the 198L-203L loop of CL to be at least 16 Å away from the nearest VL residues, 12L-14L. The 198L-203L loop is usually stabilized in part with the close association with the VL residues. The orientation of the V- and C-domain interface causes this loop to be exposed to the solvent, resulting in electron densities that are relatively weaker than those of the remainder of the Fab. The disorder of this loop is reflected by the relatively large average temperature factors, 49.3 and 45.6 Å^2 for Fab 1 and Fab 2, respectively. These values are twice that of the mean temperature factors for Fab·PCP 1, 21.5 Å^2, and for Fab·PCP 2, 22.8 Å^2 (Table I). In contrast, the compression on the H-chain portion of the molecule results in a closer interaction between VH and CH, and as a result, the 212H-217H loop of CH comes within 8 Å of the nearest residues of VH, 9H-11H.

The two Fabs in the asymmetric unit point in opposite directions and have their interfaces at the C-domains (Fig. 3). It requires a near symmetric 179.4° rotation to superimpose one Fab to the other. Because noncrystallographic symmetry restraints were not used during any stage of refinement, the r.m.s. deviation of all Cα atoms is 1.33 Å. The r.m.s. deviation is 0.97 Å when only the Cα atoms of conserved β-strand residues are used. The r.m.s. deviations of different domain superpositions are shown in Table II. These values are less than 1 Å when only the Cα atoms of conserved β-strand residues are used, which indicate that the relative positions of the constant and variable domains are different between the two Fabs and result in different elbow angles. In addition, the larger r.m.s. deviation in the constant domains is caused, in part, by the 198L-203L loop of CL (0.72 Å), as discussed above, and the 127H-133H loop in CH, for which the r.m.s. deviation is 1.78 Å. This loop has been found to be disordered in other Fab structures (29). The 127H-133H loops from the two 6B5 Fab in the asymmetric unit face each other. Although omit map calculations allowed these loops to be traced, their electron densities are relatively weak, as indicated by high average temperature factors, 37.9 Å^2 for the Fab 1 loop and 47.3 Å^2 for the Fab 2 loop.

PCP Interaction with Fab Residues—The refined structure of PCP in the Fab binding site deviates little from the crystal structure of pure PCP (21). The phenyl ring is in axial position and the piperidine ring in equatorial position, with respect to the cyclohexane ring, thus forming a "T" formation (Fig. 2). The r.m.s. deviation is 0.168 Å for PCP in Fab 1 and 0.143 Å for PCP in Fab 2 when each is compared with the crystal PCP structure. The phenyl ring has rotated in opposite directions for the two PCP molecules, by about 10° for PCP in the Fab 1 and 5° for PCP in the Fab 2. The PCP in the binding site was refined with the default potential parameters obtained from the XPLOR parameter-generating program (22), which assigned 1,000 kcal/mol Å^{-2} for bond length constants and 500 kcal/mol rad^{-2} for bond length constants. Eighty percent reduction of these constants resulted in r.m.s. deviation of greater than 0.3 Å and showed significant distortions of the PCP cyclic substituents. In contrast, increase of these parameters by 20 times resulted in the r.m.s. deviation of 0.1 Å, though the phenyl ring rotation was still evident to a smaller extent. Between these two extremes, the default parameters were judged to be reasonable for usage in these structural refinements.

The binding pocket of 6B5 Fab is about 13 Å in diameter and 13 Å deep. The PCP ligand is surrounded on all sides by aromatic and histidine residues (Fig. 4). At the bottom of the binding pocket, Phe 100H and the adjacent Phe 89L contact the cyclohexane ring of PCP. At the middle portion of PCP, the surrounding residues are Tyr 32L, His 27dL, and Tyr 96L from the L-chain and Trp 47H, His 35H, Tyr 50H, and Tyr 33H from the H-chain. The phenyl ring of PCP points toward Tyr 33H

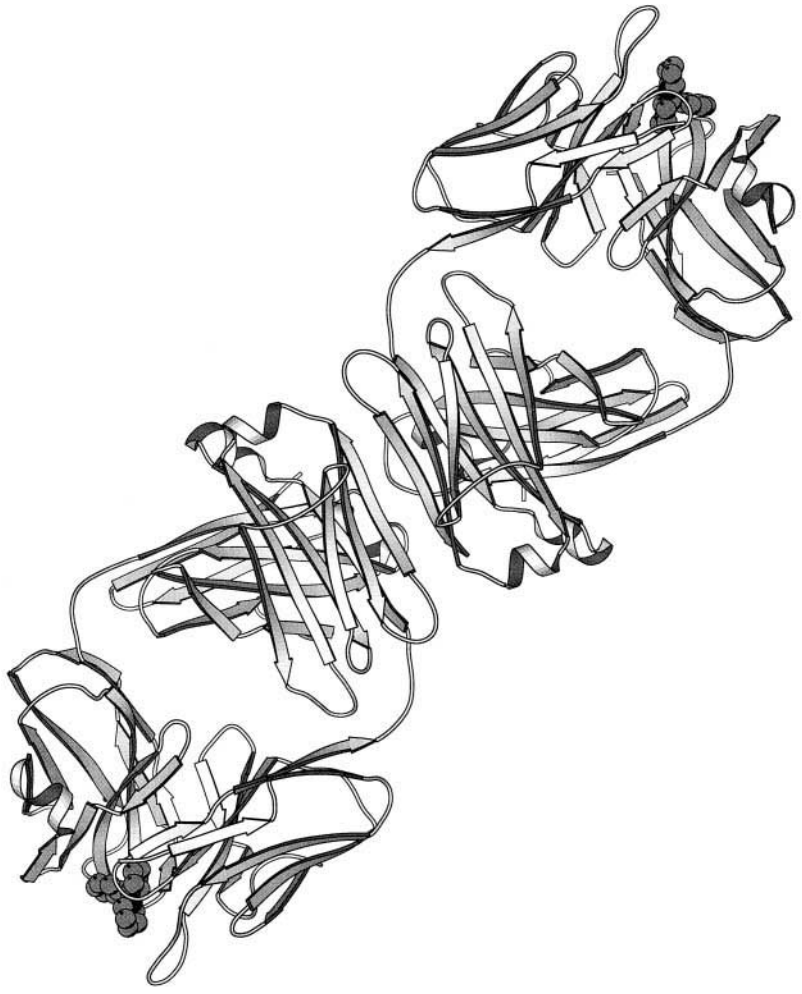

FIG. 3. **Two complexes of Fab·PCP crystal structure in asymmetric unit of *P*1 space group.** PCP is shown in *solid images* in the binding site of each Fab.

TABLE I
Data collection and refinement statistics for the 6B5 Fab-PCP structure

Data collection		Refinement	
Space group	*P*1	Resolution range	6.0–2.2
a, *b*, *c* (Å)	53.4, 67.7, 68.0	Reflections ($\|F\| > 2\ \sigma$)	31,830
α, β, γ (°)	62.1, 84.7, 83.2	Non-hydrogen, non-water atoms	6,702
Number of crystals	2	Ordered water molecules	679
Maximum resolution (Å)	2.2	R_{cryst}[b], R_{free}[c]	0.199, 0.286
Total observations ($I > 1\ \sigma$)	69,236	r.m.s. dev. bond length (Å)	0.015
		r.m.s. dev. bond angle (°)	2.4
Unique observations ($I > 1\ \sigma$)	33,694	r.m.s. dev. dihedral angle (°)	27.6
		r.m.s. dev. improper angle (°)	2.3
Completeness (%)	79.3	Ramachandran plot quality (%)[d]	
R_{merge}[a]	0.091	Fab-PCP 1	83.2, 15.9, 0.5, 0.3
$\langle I/\sigma_I \rangle$	9.8	Fab-PCP 2	84.1, 15.1, 0.5, 0.3
Last shell range	2.4–2.2	Mean temperature factor (Å^2)	
Completeness (%)	63.5	Fab-PCP 1	21.5 ± 9.3
R_{merge}	0.221	Fab-PCP 2	22.8 ± 9.2
$\langle I/\sigma_I \rangle$	3.7	Water	26.8 ± 12.0

[a] $R_{merge} = \Sigma_i(\Sigma_j|I_{ij} - \langle I_i \rangle|)/\Sigma_i\langle I_i \rangle$; I_{ij} is the scaled intensity of the *j*th observation of each unique reflection *i* and $\langle I_i \rangle$ is the mean value.
[b] $R_{cryst} = \Sigma_{hkl}||F_o| - |F_c||/\Sigma_{hkl}\ |F_o|$.
[c] R_{free} obtained from 3,074 reflections.
[d] Ramachandran plot quality compiled with the PROCHECK program (40) indicating percentages of main chain torsion angles in most favored regions, additional allowed regions, generously allowed regions, and disallowed regions, respectively.

and Tyr 50H. The side chain of His 35H is perpendicularly positioned below the phenyl ring of PCP. Positioned above, and enclosing PCP in the binding site, is Trp 97H. Polar interactions include the nitrogen atom of the PCP piperidine ring (pK_a 8.5), which is in close contact with the carbonyl oxygen atom of Gly 91L (2.9 Å) and carbonyl oxygen atom of Trp 97H (3.8 Å).

The amino acid residues that surround those interacting with PCP provide a support framework. In CDR 1L the side chains of His 27dL and Tyr 32L interact with the PCP antigen, and are stabilized by forming hydrogen bonds with Asn 28L positioned between them. Tyr 32L is additionally stabilized by Asn 30L and Asp 98H. On the H-chain side, aromatic side chains of CDR 1H and 2H residues contribute to the interaction with PCP. The Tyr 33H residue, which is in contact with the phenyl ring of PCP, is stacked on the backside with the ring of Tyr 52H. The side chain of Trp 47H does not make a direct

TABLE II
Quaternary structural analysis of 6B5 Fab

Elbow angle			
Fab 1	143°	Fab 2	139°
Pseudodyad			
Fab 1 V	176°	Fab 2 V	177°
Fab 1 C	170°	Fab 2 V	168°

Superposition between two Fabs using Cα atoms (in Å)

	All residues	β-strand residues
Variable and constant domains	1.33	0.97
VL + VH	0.49	0.37
CL + CL	1.63	0.53
VL	0.45	0.32
CL	0.84	0.49
VH	0.48	0.36
CH	1.36	0.50

contact with PCP but is close to it and is positioned between those that are, such as Tyr 96L, His 35H, and Tyr 50H.

Table III identifies the buried molecular surface areas of the PCP ligand and surrounding Fab residues. Both L and H-chain CDR 3 make significant contributions to the interaction with the ligand, in that 29% of buried surface area comes from CDR 3L and 35% from CDR 3H. CDR 3H makes the largest amount of contact with PCP, and Trp 97H is a significant contact residue with its side chain acting as an umbrella shielding PCP from the solvent. Buried surface area contributed by Trp 97H alone is 15%, more than any from the 16 residues that are in contact with PCP. Furthermore, molecular surface area of PCP complexed to Fab 1 is 252 Å^2 and that complexed to Fab 2 is 254 Å^2, and both are buried 97% by the surrounding Fab residues.

From the 679 ordered water molecules modeled in the asymmetric unit of the two 6B5 Fab·PCP structures, one water molecule was found in each binding site, buried between PCP and CDR residues. This single ordered water molecule is located on the side of cyclohexane and piperidine rings of PCP and interacts with the side chain of Glu 34L (Fig. 4).

The sequences and conformations of the CDR, except CDR 3H, are similar to those of other Fab structures. CDR 2L is shielded by CDR 1L and 3H from making a direct contact with PCP. CDR 1L in other Fab structures ranges from 10 to 17 amino acid residues in length. The relatively long CDR 1L of 6B5 (16 residues, Fig. 1) is often found in Fabs that bind small ligand molecules (30, 31).

DISCUSSION

PCP, also known as "Angel Dust," has become a widespread and dangerous drug of abuse (4). There are numerous reports of PCP inducing violent and bizarre behaviors (32). PCP can precipitate latent psychosis and a drug-induced dementia that resembles schizophrenia. Because there are no known antagonists for PCP, the treatment of the clinical problems associated with PCP overdose is very difficult. Treatment of a drug overdose is compounded by the fact that PCP has a widespread extravascular distribution and a very slow elimination from the body. Both polyclonal and monoclonal antibody (6B5) treatments of PCP toxicity in laboratory animals have proved successful (12). The use of Fab 6B5 as a PCP antagonist has resulted in a rapid reversal of PCP-induced behavioral toxicity in the rat within minutes following intravenous administration. Administration of purified Fab 6B5 to humans with PCP overdose may provide an effective and efficient treatment protocol for chemical-induced central nervous system toxicity. Knowledge of the 6B5-PCP complex as reported herein, can provide a basis for further Fab or single-chain Fv engineering to modify the pharmacokinetics and antigenicity of the protein.

The binding pocket of antibody 6B5 Fab has a concentrated amount of amino acids with aromatic side chains in the binding site as compared with other known Fabs in the Protein Data Bank, Brookhaven National Laboratory (Table III). A distinguishing feature of 6B5 is the presence and role of Trp 97H. Recent examination of the Protein Data Bank revealed only two other Fab structures with Trp in this position of the CDR 3H, TE33 (code 1tet) and R6.5 (code 1rmf). The tryptophan residue in these other Fab structures does not appear to play a critical role in the interaction with the antigen, in that the side chain of Trp 97H swings outward from the antigen binding site. Furthermore, the contact of Phe 89L with the PCP antigen indicates a very hydrophobic nature of the binding pocket of 6B5. The position 89L is next to Cys 88L in the core of VL and composed of Gln or Ser in about 70% of Fab structures, whereas Phe occurs only in about 5%. The Phe 89L residue is usually shielded from direct contact with antigen by CDR 3H residues (*e.g.* TE33), but in 6B5 it seems to play an integral part in the formation of hydrophobic binding pocket for PCP.

Fluorescence and circular dichroism (CD) spectroscopy are useful techniques to probe antibody structures and the geometric arrangements of antigen or ligand contacts with aromatic residues (33–35). We examined native 6B5 and its ligand-complexed form for changes in the intrinsic Trp or Tyr fluorescence and changes in the CD spectra and failed to detect any ligand-induced Trp or Tyr quenching, or measurable changes in chromophore absorbency in the near UV spectrum.[2] In some antibody-ligand complexes, distinct changes in both intrinsic Trp fluorescence and CD can be observed upon ligand binding, and these observations have been in agreement with the crystal structures (36). However, there were no observable changes in the intrinsic fluorescence and CD spectra of 6B5-ligand complexes as expected because of the location and direct ligand contact with Trp 97H. This suggests a high degree of solvent exposure of this residue and its orientation with respect to the ligand (*i.e.* an absence of any π-π ring stacking arrangement) may account for the absence of ligand-induced changes in the spectroscopic signature of this mAb. In contrast, in the anti-fluorescein 4–4-20 antibody, an induced CD spectra from the bound fluorescein ligand appears to be because of a direct ligand contact with several aromatic amino acids in the binding site (37). For the anti-guanidinium sweetener antibodies NC6.8 and NC10.14, changes in both intrinsic Trp fluorescence and near-UV CD were easily identified as being contributed from the Trp 33H (for NC6.8) or Trp 91L and Tyr 101H (for NC10.14) side chains that undergo π-π contacts with the *p*-cyanophenyl ring of the ligand (35).

The binding site architecture of the anti-cholera toxin peptide Fab TE33 (code 1tet) is very similar to that of 6B5 Fab (29). The CDRs of both Fabs have the same number of residues and similar amino acid composition and conformations, except CDR 3H which is one residue shorter in TE33 (sequence: ^{93}ARR-SWYF-DVW^{103}). It is also interesting to note that the elbow angle for TE33 is 142°, which is very close to that of 6B5 (Table II). Both Fabs share similar backbone conformations as the superposition of Cα atoms of conserved β-residues of combined VL-VH domain pair results in 0.58 Å r.m.s. deviation. The TE33 Fab binds a 15-residue peptide (only 12 residues reported in the 1tet structure). Its binding site is concentrated with aromatic residues nearly equivalent to that of 6B5, with small but significant changes. For example, Tyr 33H of 6B5 is replaced in TE33 by Gly, so that the side chain of Gln 5 of the peptide is inserted between the two β-strands (CDR 2H) of Fab H-chain (Fig. 5). In TE33 the NE1 atom of Trp 97H ring

[2] S. Y. Tetin and D. S. Linthicum, unpublished observations.

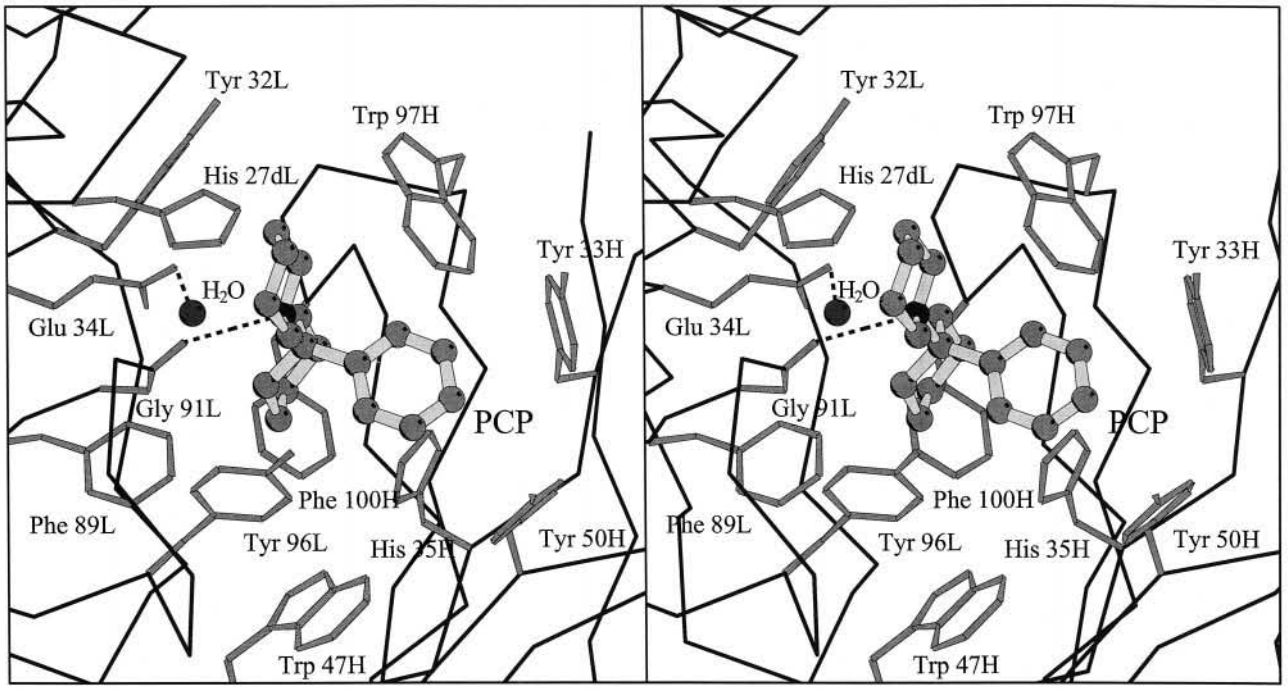

FIG. 4. **Stereo drawing of PCP in the 6B5 Fab binding site surrounded by aromatic amino acid side chains.** Also shown are the carbonyl oxygen atom of Gly 91L interacting with the lone nitrogen atom of PCP and a water molecule located adjacent to PCP in the binding pocket.

TABLE III
Buried molecular surface areas for 6B5 Fab interaction with PCP

Fab 1				Fab 2			
Residue	Area (Å^2)	% Area	Total CDR % area	Residue	Area (Å^2)	% Area	Total CDR % area
His-27dL	18	6.1		His-27dL	12	4.5	
Tyr-32L	22	7.8		Tyr-32L	18	6.8	
Glu-34L	4	1.4	CDR 1L 15.3	Glu-34L	4	1.4	CDR 1L 12.7
Phe-89L	12	4.2		Phe-89L	16	6.0	
Gly-91L	33	11.4		Gly-91L	21	8.1	
Thr-92L	8	2.8		Thr-92L	5	2.0	
Tyr-96L	31	10.5	CDR 3L 28.9	Tyr-96L	33	12.7	CDR 3L 28.8
Tyr-33H	17	5.8		Tyr-33H	18	6.7	
His-35H	25	8.7	CDR 1H 14.5	His-35H	22	8.2	CDR 1H 14.9
Tyr-50H	17	5.9	CDR 2H 5.9	Tyr-50H	16	6.2	CDR 2H 6.2
Ser-95H	14	4.8		Ser-95H	13	4.9	
Thr-96H	5	1.8		Thr-96H	7	2.6	
Trp-97H	45	15.5		Trp-97H	40	15.0	
Asp-98H	16	5.6		Asp-98H	12	4.6	
Asp-99H	9	3.2		Asp-99H	14	5.4	
Phe-100H	13	4.5	CDR 3H 35.4	Phe-100H	13	4.9	CDR 3H 37.4
Total	289			Total	264		
PCP 1	245	97.2		PCP 2	247	97.2	

provides a hydrogen-bond with carbonyl oxygen atom of Ile 7 of the peptide, as the C terminus of the peptide antigen point away from the TE33 Fab binding site. An interesting feature of this Fab is the placement of Arg 95H that forms a salt bridge with Glu 34L. This is in contrast with 6B5, in which the long side chain of Arg 95H is replaced by Ser, so that the PCP ligand can be positioned in the corresponding space occupied by the Arg 95H side chain in TE33, as shown in Fig. 5. In 6B5, Glu 34L interacts with Asp 99H on the opposite side of CDR 3H loop from residue 95H. Thus, based on a framework of aromatic residues that remains essentially unchanged, the replacement of a few key residues in the binding site can alter the geometry of ligand contacts, thereby resulting in an antibody with completely different antigen specificity.

Another Fab with the same CDR lengths as TE33, but different amino acid composition, is Jel-103, which binds RNA (Protein Data Bank code 1mrd) (38). In Jel-103, the RNA antigen is not placed deep in the binding pocket, which is mainly because of the Arg 96L that is positioned below the RNA antigen, and the RNA ring is stacked with Tyr 32L. In 6B5, Tyr 32L is in contact with the piperidine ring of PCP, and Tyr 96L is positioned to the side of PCP. Thus, the PCP antigen is allowed to be positioned deeper in the binding pocket. The Trp 97H residue in 6B5 is occupied by Arg in Jel-103, and its side chain is arched toward the RNA to permit direct contacts with the antigen. The Arg residues in these structures play very different roles in the binding site.

The hapten used for generating the anti-PCP mAb 6B5 (*i.e.* PCHAP) was chosen based on previous polyclonal antibody ligand specificity studies (9). For these studies, anti-PCP rabbit polyclonal antibodies were generated using a series of five PCP-like haptens conjugated to protein carrier. Only the PCHAP hapten generated antibodies with a ligand reactivity profile that mimicked the known pharmacological activity profile

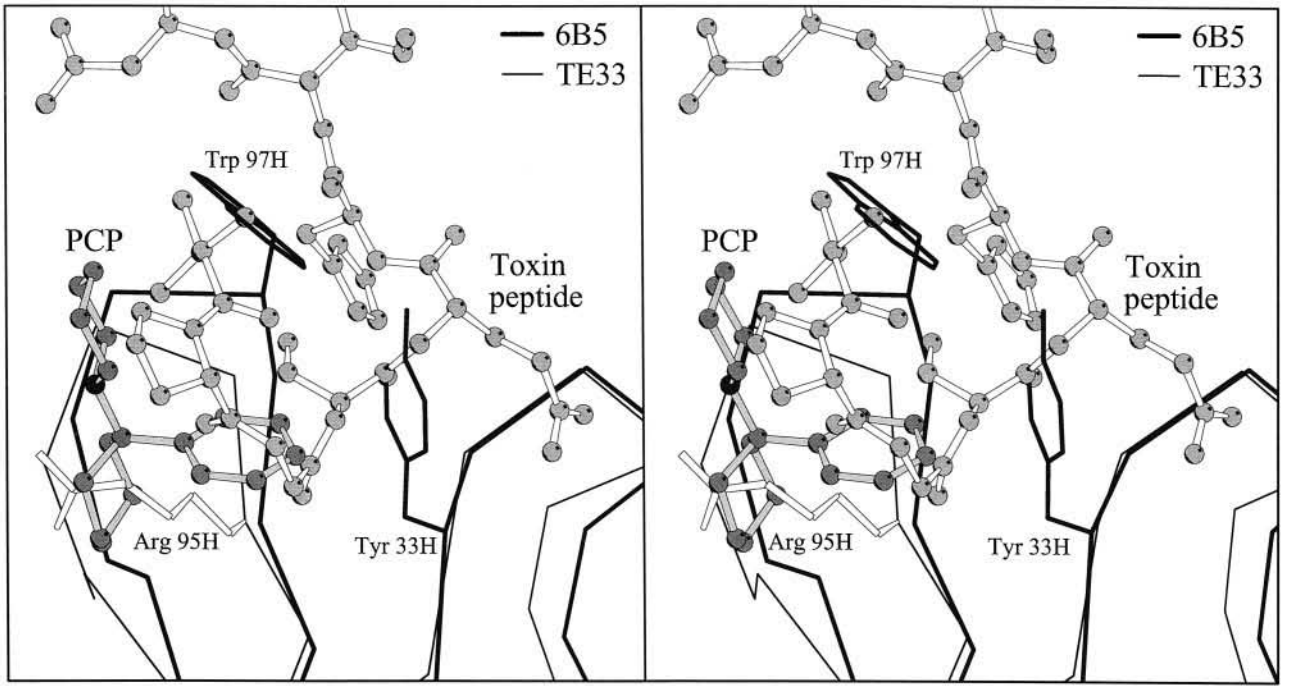

FIG. 5. **Comparison of PCP binding to 6B5 Fab and cholera toxin peptide binding to TE33 Fab (29).** The two structures are superpositioned to indicate that the two Fab binding sites with a similar framework can accommodate the different types of antigen molecules by replacements of amino acid substitutions at key positions. For the larger cholera toxin peptide to bind, Tyr 33H of 6B5 is changed to Gly in TE33. Also, the Trp 97H side chain is positioned above the PCP antigen in 6B5; however, this side chain ring is turned away from the center of the binding site to allow for the positioning of the peptide antigen in TE33. In addition, Arg 95H in TE33 is changed to serine in 6B5 so that the PCP antigen is allowed to be inserted deeper into the binding site.

of the central nervous system PCP receptor (*i.e.* the *N*-methyl-D-aspartate ion-gated channel). Antibody 6B5 has a ligand binding profile for arylcyclohexylamines that correlates with pharmacological activity (10).

A comparison of the structural features of the PCP binding site of 6B5 with that of the *N*-methyl-D-aspartate ion-gated channel could prove useful. The molecular determinants of the PCP binding site in the M2 segment of the oligomeric channel has been examined by site-directed mutagenesis using the glutamate receptor GluR1 (39). The PCP binding site is located in a hydrophobic transmembrane segment of the M2 chain, and binding of PCP acts to keep the channel open. Three specific point mutations in the M2 region appear to confer PCP binding specificity. Residues such as Trp-577 and Trp-593 appear to be essential to PCP binding, but residues such as Thr-582 and Ala-610 also appear to play critical roles. Thus, the geometry of residues Trp-577, Trp-593, Thr-582, and Ala-610 in the ion-gated channel site may be similar to those in 6B5, especially with respect to ligand contacts and binding specificity for related psychoactive arylcyclohexylamines.

Acknowledgments—We thank Dr. Denise Rozwarski for assistance and Dr. Sergey Tetin for assistance with the spectroscopy experiments.

REFERENCES

1. Poljak, R. J., Amzel, L. M., Chen, B. L., Phizackerley, R. P., and Saul, F. (1973) *Proc. Natl. Acad. Sci. U. S. A.* **70,** 3305–3310
2. Davies, D. R., and Metzger, H. (1983) *Annu. Rev. Immunol.* **1,** 87–117
3. Padlan, E. A. (1994) *Mol. Immunol.* **31,** 169–217
4. Burns, R. S., and Lerner, S. E. (1976) *Clin. Toxicol.* **9,** 477–501
5. Fauman, M. A., and Fauman, B. J. (1979) *Am. J. Psychiatry* **136,** 1584–1586
6. Zukin, S. R., and Zukin, R. S. (1979) *Proc. Natl. Acad. Sci. U. S. A.* **76,** 5372–5376
7. Vignon, J., Vincent, J. P., Bidard, J. N., Kamenka, J.-M., Geneste, P., Monier, S., and Lazdunski, M. (1982) *Eur. J. Pharmacol.* **81,** 531–542
8. Chaudieu, I., Vignon, J., Chicheportiche, M., Kamenka, J.-M., Trouiller, G., and Chicheportiche, R. (1989) *Pharmacol. Biochem. Behav.* **32,** 699–705
9. Owens, S. M., Zorbas, M., Lattin, D. L., Gunnell, M., and Polk, M. (1988) *J. Pharmacol. Exp. Ther.* **246,** 472–478
10. Hardin, J. S., Wessinger, W. D., Proksch, J. W., and Owens, S. M. (1998) *J. Pharmacol. Exp. Ther.* **285,** 1113–1121
11. McClurkan, M. B., Valentine, J. L., Arnold, L., and Owens, S. M. (1993) *J. Pharmacol. Exp. Ther.* **266,** 1439–1445
12. Valentine, J. L., Mayersohn, M., Wessinger, W. D., Arnold, L. W., and Owens, S. M. (1996) *J. Pharmacol. Exp. Ther.* **278,** 709–716
13. Cook, C. E., Brine, D. R., Jeffcoat, A. R., Hill, J. M., Wall, M. E., Perez-Reyes, M., and Di Guiseppi, S. R. (1982) *Clin. Pharmacol. Ther.* **31,** 625–634
14. Otwinowski, Z., and Minor, W. (1997) *Methods Enzymol.* **276,** 307–326
15. Brunger, A. T., Leahy, D. J., Hynes, T. R., and Fox, R. O. (1991) *J. Mol. Biol.* **221,** 239–256
16. Matthews, B. W. (1968) *J. Mol. Biol.* **33,** 491–497
17. Navaza, J. (1994) *Acta Crystallogr. Sec. A* **50,** 157–163
18. Jones, T. A., Zou, J., Kjelgaard, M., and Cowan, S. W. (1991) *Acta Crystallogr. Sec. A* **47,** 110–119
19. Sanger, F., Nicklen, S., and Coulson, A. R. (1977) *Proc. Natl. Acad. Sci. U. S. A.* **74,** 5463–5467
20. Cohen, G. H., Sherfiff, S., and Davies, D. R. (1996) *Acta Crystallogr. Sec. D* **52,** 315–326
21. Argos, P., Barr, R. E., and Weber, A. H. (1970) *Acta Crystallogr. Sec. B* **26,** 53–61
22. Kleywegt, G. J. (1995) *ESF/CCP 4 Newsletter* **31,** 45–50
23. Kleywegt, G. J., and Jones, T. A. (1997) *Methods Enzymol.* **277,** 208–230
24. Kabat, E. A., Wu, T. T., Perry, H. M., Gottesman, K. S., and Foeller, C. (1991) *United States DHHS,* NIH Publication 91–3242
25. Wilson, I. A., and Stanfield, R. L. (1994) *Curr. Opin. Struct. Biol.* **4,** 857–867
26. Connolly, M. L. (1983) *J. Appl. Crystallogr.* **16,** 548–558
27. Stanfield, R. L., Takimoto-Kamimura, M., Rini, J. M., Profy, A. T., and Wilson, I. A. (1993) *Structure* **3,** 83–93
28. Herron, J. N., Terry, A. H., Johnston, S., He, X.-M., Guddat, L. W., and Voss, E. W., Jr. (1994) *Biophys. J.* **67,** 2167–2183
29. Shoham, M. (1993) *J. Mol. Biol.* **232,** 1169–1175
30. Vargas-Madrazo, E., Lara-Ochoa, F., and Almagro, J. C. (1995) *J. Mol. Biol.* **254,** 497–504
31. Al-Lazikani, B., Lesk, A. M., and Chothia, C. (1997) *J. Mol. Biol.* **273,** 927–948
32. Aniline, O., and Pitts, F. N., Jr. (1982) *CRC Crit. Rev. Toxicol.* **10,** 145–177
33. Dandliker, W. B., and Levison, S. A. (1967) *Immunochem.* **5,** 171–183
34. Droupadi, P. R., Anchin, J. M., Meyers, E. A., and Linthicum, D. S. (1992) *J. Mol. Recog.* **5,** 173–179
35. Tetin, S. Y., and Linthicum, D. S. (1995) *Biochemistry* **35,** 1258–1264
36. Guddat, L., Shan, L., Anchin, J., Linthicum, D. S., and Edmundson, A. B. (1994) *J. Mol. Biol.* **236,** 247–274
37. Tetin, S. Y., Mantulin, W. W., Denzin, L. K., Weidner, K. M., and Voss, E. W., Jr. (1992) *Biochemistry* **31,** 12029–12034
38. Pokkuluri, P. R., Bouthillier, F., Li, Y., Kuderova, A., Lee, J., and Cygler, M. (1994) *J. Mol. Biol.* **243,** 283–297
39. Ferrer-Montiel, A. V., Sun, W., and Montal, M. (1995) *Proc. Natl. Acad. Sci. U. S. A.* **92,** 8021–8025
40. Laskowski, R. A., Rullman, J. A., MacArthur, M. W., Kaptein, R., and Thornton, J. M. (1996) *J. Biomol. NMR* **8,** 477–486
41. Kraulis, P. (1991) *J. Appl. Crystallogr.* **24,** 946–950